Collisionless Shock Wave Generation in Counter-Streaming Plasmas Using Gekko XII HIPER Laser*)

Takao IDE, Youichi SAKAWA[1)], Yasuhiro KURAMITSU[1)], Taichi MORITA[2)], Hiroki TANJI, Kento NISHIO[2)], Tsunehiko KATO[1)], Naofumi OHNISHI[3)], Christopher D. GREGORY[4)], Nigel WOOLSEY[4)], Alexandra DIZIERE[5)], Michel KOENIG[5)], Shoujun WANG[6)], Quanli DONG[6)], Yutong LI[6)] and Hideaki TAKABE[1)]

Graduate School of Engineering, Osaka University, 2-1 Yamada-oka, Suita 565-0871, Japan
[1)]*Institute of Laser Engineering, Osaka University, 2-6 Yamada-oka, Suita 565-0871, Japan*
[2)]*Graduate School of Science, Osaka University, 1-1 Machikaneyama, Toyonaka 560-0043, Japan*
[3)]*Graduate School of Engineering, Tohoku University, 6-6-1 Aramaki-Aza-Aoba, Aoba-ku, Sendai 980-8579, Japan*
[4)]*Department of Physics, University of York, Heslington, York, YO10 5DD, UK*
[5)]*LULI Ecole polytechnique, 91128 Palaiseau Cedex, France*
[6)]*Institute of Physics, Chinese Academy of Sciences, Beijing 100190, China*

(Received 22 December 2010 / Accepted 11 March 2011)

Collisionless shock wave generation in counter-streaming plasmas for several target materials (Al, C, Cu, and Pb) is investigated using a high-power laser system. Counter-streaming plasmas are produced by irradiating an inner surface of a double-plane target. For Al, C, and Pb, a shock wave is observed in self-emission measurements similar to the previous experiment using a CH target [Y. Kuramitsu *et al.*, J. Phys.: Conf. Series. **24**, 042008 (2010)], and the width of the transition region is much shorter than the ion-ion collision mean-free-paths. The mean-free-paths tend to be longer for heavier materials, because the ionization degrees Z are not so different among these materials.

Keywords: colissionless shock, laser plasma, laboratory astrophysics

DOI: 10.1585/pfr.6.2404057

1. Introduction

The laboratory simulation of astrophysical phenomenon has been tried to perform for many years. Dynamic astrophysical processes have mainly been studied by observation and computational simulation. The advantages of laboratory experiments are that we can control and vary the initial conditions of the physical processes. Physics of cosmic ray acceleration is one of the unsolved problems in astrophysics. It is speculated that cosmic rays whose energy is less than 10^{15} eV are accelerated at collisionless shocks in supernova remnants (SNRs) in our galaxy according to observation of x-rays [1, 2]. Therefore collisionless shock waves are one of the most important subjects in astrophysics, and they have been studied theoretically and numerically for many years. Experimental researches have also been carried out using a double-plasma device [3–5] and high-power laser systems [6–12]. A bow shock has been generated by placing a solid obstacle in the path of high-velocity laser ablation plasma [6]. Collisionless interaction has been studied in laser-produced counter-streaming plasmas with an external magnetic field to demonstrate the shocks of SNRs [7, 8]. The theoretical work by Sorasio *et al.* [13] has shown that a high Mach-number shock wave can be generated in counter-streaming plasmas with different temperatures and densities numerically using particle-in-cell (PIC) simulation and theoretically. Kuramitsu *et al.* [9] and Morita *et al.* [10] have reported collisionless shock formation in counter-streaming plasmas with a double-plane target produced by high-power laser systems. In these experiments, the material of the targets was only CH (plastic) because of low mass number [9, 10].

In this paper, We report target material dependence of shock wave generation. We used targets made of different materials (C, Al, Cu, and Pb) with different atomic number and mass.

2. Experiment

The experiment was performed with Gekko XII HIPER laser system at Institute of Laser Engineering, Osaka University. There are nine main beams in which the energy is about 120 J/beam in 351 nm (3ω) and pulse length is 500 ps. The target we used in this experiment is a double-plane target as shown in Fig. 1. We put two planes parallel, and the material of two planes of each target is

author's e-mail: ide-t@ile.osaka-u.ac.jp
*) This article is based on the presentation at the 20th International Toki Conference (ITC20).

identical. The size of each plane is 3 mm×3 mm, the thickness is 100 µm, and the separation between two planes is 4.5 mm. We used not only CH targets [9,10] but also C, Al, Cu and Pb targets. The target normal is aligned 30 degrees from the laser axis. One of the nine beams is focused on the inner surface of the 1st plane with 300 µm in diameter (intensity is 3.4×10^{14} W/cm^2), and ablation plasma is formed from the 1st plane. Almost at the same time, a plasma from the 2nd plane is created by radiation from the ablation plasma. In this way, counter-streaming plasmas are generated, and shock waves are formed by an interaction of these plasmas. We also used the targets without the 2nd plane (single-plane target) as a reference data. Figure 2 shows schematic of the experiment setup. The interaction of plasmas is diagnosed with a probe laser (Nd:YAG laser; wavelength is 532 nm and duration time is ∼14 ns) and with self-emission. Using the probe laser we obtained two-dimensional information of density by shadowgraphy with intensified charge coupled device (ICCD) cameras (200 ps gate width) and Nomarski interferometry with gated optical imager (GOI) (250 ps gate width). We also measured one-dimensional time evolution of the plasma by streaked interferometry with a streak camera. The self-emission was gated at the wavelength of 450 nm using interference filters. We obtained two-dimensional image of the self-emission with ICCD cameras (1.6 ns gate width) and one-dimensional time evolution with a streak camera, which is called streaked optical pyrometer (SOP).

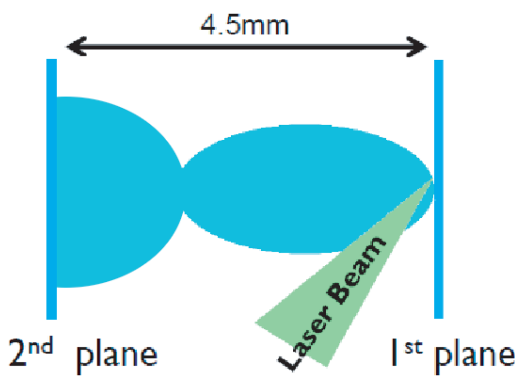

Fig. 1 Schematic view of the target design. A main laser beam is focused on the 1st plane. Two planes are made of the same material.

3. Results

SOP images for different materials are shown in Figs. 3 (a)-3 (d), where the 1st plane is at $x = 0$ mm, the 2nd plane is at $x \sim 4.5$ mm, and the time $t = 0$ ns is the peak timing of the main laser. As shown in Fig. 3, strong emission at the 1st-plane plasma ablated by the main laser and weaker emission at the 2nd-plane plasma ablated by the radiation from the 1st-plane plasma are observed at the laser timing. This means that counter-streaming plasmas are formed. Early in time, two plasmas expand from each plane. At $t = 10 \sim 20$ ns, sharp emission profiles marked with dotted lines start to appear as a result of interaction of the two plasmas except for Cu target. Figure 4 represents line profiles of self-emission for Al target shown in Fig. 3 (b) at t = 13.6, 16.6, 19.5, and 22.5 ns. The structure marked with dotted line in Fig. 3 (b) corresponds to discontinuous part of line profile (marked with arrows) in Fig. 4, and the line profiles become steeper in time. Similar steepening in emission profile was reported by Kuramitsu for CH double-plane targets [9]. Furthermore, a snapshot of shadowgraphy showed a filament, which indicating a large density jump, at the same position as the sharp emission, and it was concluded that the observed emission profile was a shock wave [9]. We also obtain the steepening of the line profile for C and Pb targets. Therefore, the sharp emission profiles indicated by dotted lines in Fig. 3 represent shock waves. Formation times and velocities of the shock

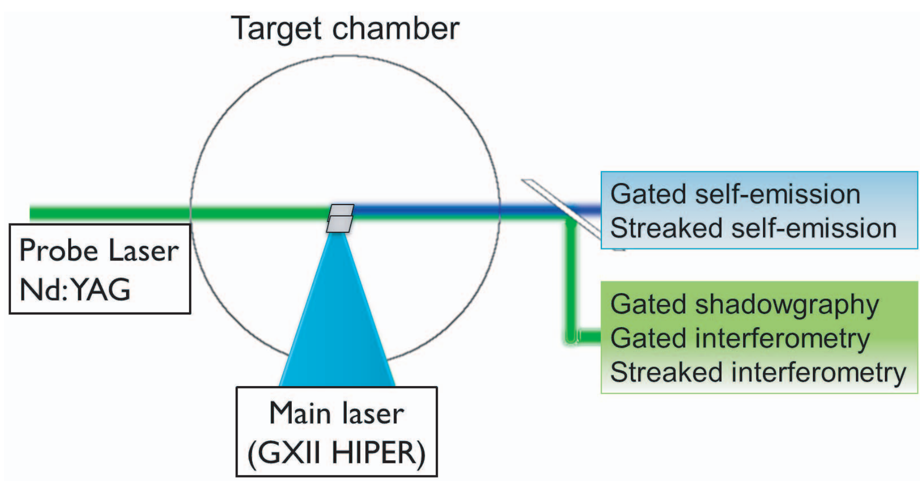

Fig. 2 Experimental setup. The green line is the path of probe YAG laser and the blue line from target chamber center (TCC) is the path of self-emission at the wavelength of 450 nm.

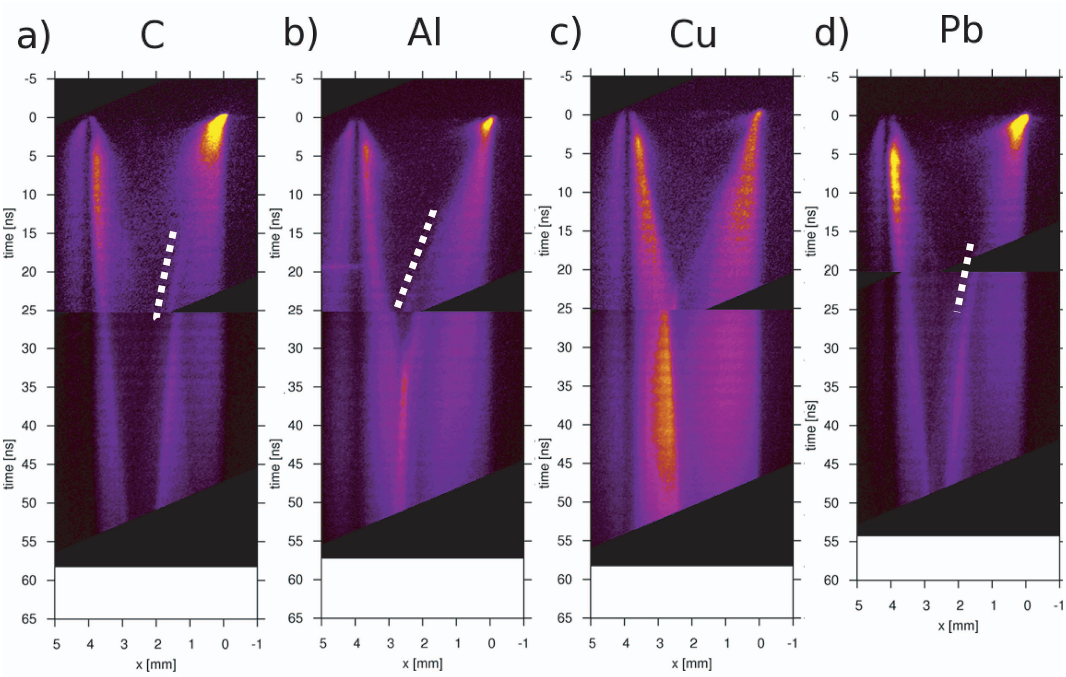

Fig. 3 Streaked self-emission optical pyrometer(SOP) taken from 5 ns before laser timing. X axis is distance and y axis is time. Material of the target is (a) C, (b) Al, (c) Cu, and (d) Pb.

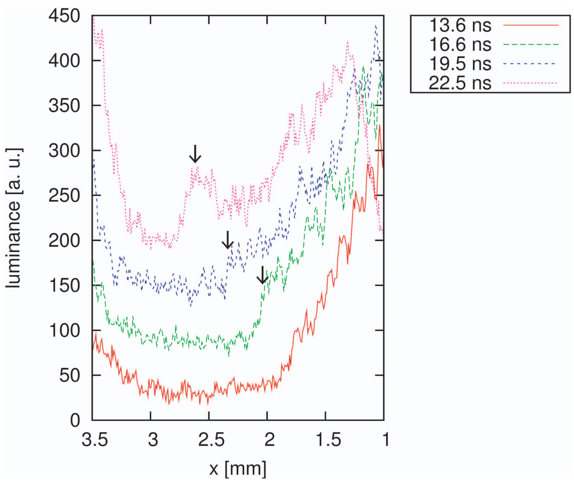

Fig. 4 Line profile of the luminance of Al target.

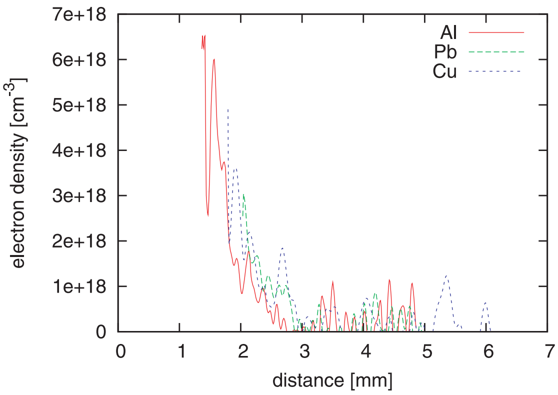

Fig. 5 Density distribution of the single-plane target made of some materials. X axis is the distance form the surface of the 1st plane.

wave are shown in Table 1. They are different among target materials, but no clear dependence on neither mass nor atomic number are found. On the other hand, we could not observe such a shock structure for Cu target. In the case of Cu, the emission intensity near the 2nd-plane plasma was kept strong, while that of the other materials decreased. It indicates that a shock wave could be generated on the 2nd-plane plasma.

Figure 5 shows the electron number density distribution obtained from two-dimensional interferometry for single-plane targets. We could not derive density profile for double-plane targets because the images were so complicated that we could not identify the fringes. According to Fig. 5, the electron densities at 2 ~ 3 mm away from the 1st plane are $\sim 10^{18}\,\mathrm{cm}^{-3}$ or less for all the materials. Table 1 shows some quantities of the shock waves for each target obtained from Fig. 3 and hydrodynamic simulations.

Ion-ion collision mean-free-path λ_{ii} is expressed as [14],

$$\lambda_{\mathrm{ii}} = \frac{2\pi\epsilon_0^2 m_{\mathrm{i}}^2 v^4}{n_{\mathrm{i}} Z^4 e^4 \ln\Lambda}, \qquad (1)$$

where m_{i} is the ion mass, v is the relative velocity of counter-streaming plasmas, Z is the ionization degree, e is the elementary charge, ϵ_0 is the vacuum permittivity, and $\ln\Lambda$ is the Coulomb logarithm. We used one-dimensional hydrodynamic simulation ILESTA to estimate Z at typi-

Table 1 Measured and calculated plasma parameters.

Material	CH	C	Al	Cu	Pb
Mass number A	7.5	12	27	64	207
Atomic number	3.5	6	13	29	82
Calculated ionization degree Z	3.5	6	~7	~7	~5
Shock velocity [km/s]	45	64	106	-	25
Typical time of shock formation [ns]	13	10	15	-	18 ~ 20
$v = v_{up} - v_{down}$ [km/s]	229	306	200	-	158
Mean-free-path λ_{ii} [mm]	0.49	2.5	1.5	70 (typical)	77
Shock width [mm]	0.1	0.1	0.08	-	0.2

cal time t when the shock waves are generated and $x = 2 \sim 3$ mm. We calculate the velocity of the fluid that starts moving from the target at the laser timing and comes to the shock when the shock wave was generated [10]. The relative velocity of counter-streaming ions v as a function of time t and position x is calculated as

$$v = v_{up} - v_{down} = \frac{d - x}{t} - \left(-\frac{x}{t}\right) = \frac{d}{t}, \qquad (2)$$

where v_{up} and v_{down} are the velocities at upstream and downstream regions of shock wave, respectively, and $d = 4.5$ mm is the separation between two planes. v is independent of x and determined simply by t. We used $n_e = 10^{18}$ cm^{-3} and shock formation time for t. The calculated λ_{ii} for all the materials are much larger than the width of the transition region of the shock wave. Therefore, these shock waves we observed are collisionless shock waves. Furthermore, mean-free-paths of heavier materials become longer because the calculated values of Z for C, Al, and Pb vary only within a factor of two. Therefore, it is easy to create collisionless shock wave using heavier materials.

4. Conclusions

Counter streaming plasmas are produced by irradiating double-plane targets made of Al, C, Cu, and Pb with Gekko XII HIPER laser system. We obtain the steepening of the line profile of self-emission for C, Al, and Pb. These sharp emission profiles represent shock wave similar to the previous experiment using CH targets [9]. The width of the transition region of the shock wave is much shorter than the ion-ion collision mean-free-path λ_{ii}. Mean-free-paths of heavier materials tend to be longer because the calculated values of Z for these materials are not so different; the heavier-material targets are easier to satisfy the collisionless condition. We observed the difference in shock speed for different material target, but could not find clear dependence on mass or atomic number of target materials.

[1] F.A. Aharonian *et al.*, Nature (London) **432**, 75 (2004).
[2] Y. Uchiyama *et al.*, Nature (London) **449**, 576 (2007).
[3] R.J. Taylor *et al.*, Phys. Rev. Lett. **24**, 206 (1970).
[4] H. Ikezi *et al.*, Phys. Fluids **16**, 2167 (1973).
[5] H. Ikezi *et al.*, Phys. Rev. Lett. **36**, 794 (1976).
[6] A.R. Bell *et al.*, Phys. Rev. A **38**, 1363 (1988).
[7] C. Coutois *et al.*, Phys. Plasmas **11**, 3386 (2004).
[8] N.C. Woolsey *et al.*, Plasma Phys. Control. Fusion **46**, B397 (2004).
[9] Y. Kuramitsu *et al.*, Journal of Physics: Conference Series **244**, 042008 (2010).
[10] T. Morita *et al.*, Phys. Plasmas **17**, 122702 (2010).
[11] L. Romagnani *et al.*, Phys. Rev. Lett. **101**, 025004 (2008).
[12] P.M. Nilson, *et al.*, Phys. Rev. Lett. **103**, 255001 (2009).
[13] G. Sorasio, *et al.*, Phys. Rev. Lett. **96**, 045005 (2006).
[14] L. Spitzer, Jr., *Physics of Fully Ionized Gases* (Interscience Publishers, New York, 1959).